ARTICLE

Zinc(II) and Mercury(II) Complexes of Pyrazole-Based NNN-Type Ligands: Syntheses, X-ray Structures, Thermal Analyses and DFT Studies

Çiğdem Hopa,*[a] Raif Kurtaran,[a] Akın Azizoğlu,[a] Mahir Alkan,[a] N. Burcu Arslan,[b] and Canan Kazak[b]

Abstract. Monomeric zinc(II) and mercury(II) complexes containing tripodal nitrogen donor ligand 2,6-bis(3,4,5-trimethyl-*N*-pyrazolyl)pyridine (btmpp) were synthesized, and characterized by elemental and spectroscopic (IR, UV/Vis) analyses, TG-DTA and single-crystal X-ray diffraction studies. X-ray analyses of the complexes [Zn(btmpp)Cl₂] (**2**) and [Hg(btmpp)(SCN)₂] (**3**) showed that both structures crystallize in space group $P2_1/c$ with $a = 7.9722(6)$, $b = 18.3084(13)$, $c = 13.3117(9)$ Å and $Z = 4$ for **2** and $a = 8.7830(3)$, $b =$ 21.1489(7), $c = 12.0682(4)$ Å and $Z = 4$ for **3**. Both monomeric units contain pentacoordinate metal ions in distorted square-pyramidal arrangement. The structures of complexes **2** and **3** were also computed with DFT methods at B3LYP/LanL2DZ level and are in good agreement with the experimental values obtained from X-ray analysis. The NPa charge distributions, HOMO–LUMO gaps, and dipole moments for **1**, **2**, and **3** were also reported. Natural bond orbital analyses were performed to reveal local charges and charge transfers in **1**, **2**, and **3**.

Introduction

Over the last two decades, there has been an increasing interest in metal complexes of pyrazole-derived ligands, mainly due to their potential application as building blocks for supramolecular assemblies,[1] photovoltaic solar cell,[2] their capabilities to serve as catalysts of organic reactions,[3] spin-crossover compounds,[4,5] luminescence properties,[6] and biological models.[7] In this context, *Zhao* and co-workers synthesized a new bis-pyrazole derivative planar tridentate ligand 2,6-bis(5-phenyl-1H-pyrazol-3-yl)pyridine (H₂BPPP) and its zinc and cadmium metal complexes and additionally investigated their luminescence properties. Also, *Willison* et al.[8] reported platinum(II) 2,6-bis(N-pyrazolyl)pyridine complexes, and investigated their luminescence properties.

In recent years, density functional theory (DFT) has been favored as a tool for quantum chemistry. DFT methods such as B3LYP/6-31G(d) are often considered to be a standard model chemistry for many applications.[9]

As a part of our systematic studies of the coordination chemistry with btmpp, we recently published a mononuclear Fe^III complex[10] and a chlorido-bridged Cd^II-isothiocyanato complex.[11] Complexes of Group 12 metal ions, such as zinc(II) and mercury(II) are also of interest since they are involved in many biological processes.[12,13] In this paper, we report on the synthesis and the spectral, thermal, and X-ray single crystal structural analyses of two new mononuclear complexes, [Zn(btmpp)Cl₂] (**2**) and [Hg(btmpp)(SCN)₂] (**3**) (Figure 1). We also calculated the structural parameters of complexes **2** and **3** in the ground state to compare the results with the DFT methods.
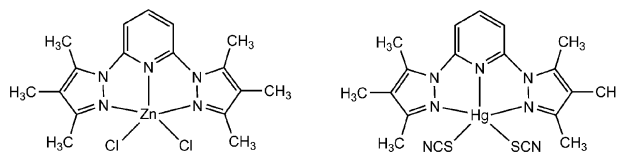

Figure 1. Chemical structures of the complex **2** and **3**.

Experimental Section

Materials and Measurements

All reagents and solvents were purchased from Merck, Aldrich or Carlo Erba and were used without further purification. The elemental analyses for the ligands and complexes were carried out with a Leco, CHNS-932 analyzer. Melting points were measured using Stuart Melting Point SMP3. The IR spectra were obtained by using IR grade KBr disks with a Perkin–Elmer 1600 Series FTIR spectrophotometer in the range of 4000–400 cm⁻¹. The electronic spectra were obtained using a Perkin–Elmer Lambda 25 UV/Vis spectrophotometer. The thermogravimetry/differential thermal analysis (TG/DTA) measurements were run with a Perkin–Elmer Diamond DTA/TG thermal analyzer. In this study, thermogravimetric curves were obtained with a carrier gas flow rate of 200 mL·min⁻¹ and a heating rate of 20 °C·min⁻¹ under nitrogen (3 bar) in ceramic crucibles. The experiments were carried out in a temperature range of 30–1000 °C.

* Dr. Ç. Hopa
  E-Mail: cigdem@balikesir.edu.tr
[a] Department of Chemistry
  Faculty of Arts and Sciences
  Balıkesir University
  Cagis 10145, Balıkesir, Turkey
[b] Department of Physics
  Faculty of Arts and Sciences
  Ondokuz Mayıs University
  55139, Samsun, Turkey

Syntheses

btmpp (1): The ligand btmpp was prepared by heating a mixture of 2,6-dichloropyridine and the sodium salt of 3,4,5-trimethyl-*N*-pyrazole in diglyme under reflux.[10] 3,4,5-Trimethylpyrazole was synthesized by the reaction of hydrazine hydrate and 3-methyl-2,4-pentanedione.[11]

[Zn(btmpp)Cl$_2$] (2): A solution of 2,6-bis(3,4,5-trimethyl-*N*-pyra-zolyl)pyridine (btmpp) (0.266 g, 1 mmol) in hot ethanol (20 mL) was added to a hot ethanol solution (20 mL) of $ZnCl_2$ (0.136 g, 1 mmol). The mixture was filtered off while the solution was hot. The resulting mixture was set aside for three days and fine colorless crystals formed. The crystals were filtered off and dried in air. Yield: 74 %, ^{1}H NMR (400 MHz, 298 K, $(CD_3)_2SO$) 1.94 (s, 3 H), 2.19 (s, 3 H), 2.51 (s, 6 H), 3.35 (s, 6 H), 7.63 (d, 2 H, $J = 8.04$ Hz), 8.04 (t, 1 H, $J = 7.56$ Hz). ^{13}C NMR (100 MHz, 298 K, $(CD_3)_2SO$) 7.63, 11.77, 12.10, 112.54, 115.07, 136.70, 141.34, 149.03, 149.72. Anal. Calc. For $C_{17}H_{21}Cl_2N_5Zn$: C, 47.26; H, 4.86; N, 16.22. Found: C, 46.85; H, 4.72; N, 16.09. Suitable crystals were selected for the XRD study.

[Hg(btmpp)SCN$_2$] (3): A solution of 2,6-bis(3,4,5-trimethyl-*N*-pyra-zolyl)pyridine (btmpp) (0.266 g, 1 mmol) in hot ethanol (20 mL) was added to a hot ethanol solution (20 mL) of $Hg(SCN)_2$ (0.316 g, 1 mmol). The mixture was filtered off while the solution was hot. The resulting mixture was set aside for a few days and fine colorless crys-tals formed. The crystals were filtered off and dried in air. Yield: 67 %, mp: 180 °C, ^{1}H NMR (500 MHz, 298 K, $(CD_3)_2SO$) 1.95 (s, 3 H), 2.22 (s, 3 H), 2.51 (s, 6 H), 3.34 (s, 6 H), 7.66 (d, 2 H, $J = 8.08$ Hz), 8.10 (t, 1 H, $J = 8.08$ Hz). ^{13}C NMR (100 MHz, 298 K, $(CD_3)_2SO$) 7.64, 11.73, 12.10, 112.87, 115.53, 115.96, 137.31, 141.89, 149.41, 149.89. Anal. Calc. For $C_{19}H_{21}N_7S_2Hg$: C, 37.25; H, 3.43; N, 16.01. Found: C, 37.08; H, 3.31; N, 15.88. Suitable crystals were selected for the XRD study.

X-ray Structure Determination

One of the fine colorless single crystals was mounted on a glass fiber and the intensity data of the Zn[II] and Hg[II] complexes were collected using a STOE IPDS 2 diffractometer (Mo-K_α radiation, $\lambda = 0.71073$ Å) at 293 K. The structures (Figure 2 and Figure 3) were solved by direct methods using SHELXS-97[14] and refined by a full-matrix least-squares procedure (SHELXL-97).[14] All non-hydrogen atoms were easily found from the difference Fourier map and refined anisotropi-cally. All hydrogen atoms of **2** and **3** were refined freely. The molec-ular plots were prepared by using ORTEPIII.[15] The details of data collection, refinement and crystallographic data are summarized in Table 1. Crystallographic data for the structures of **2** and **3** reported in this paper have been deposited with the Cambridge Crystallo-graphic Data Centre (The Director, CCDC, 12 Union Road, Cam-bridge, CB2 1EZ, UK; E-Mail: deposit@ccdc.cam.ac.uk; www: http://www.ccdc.cam.ac.uk; Fax: +44-1223-336033) and are available free of charge on request, quoting the deposition number respectively CCDC-693635 and CCDC-693636.

Computational Methods

The structure of molecules, **2** and **3**, as determined by X-ray crystal structure analysis, were fully optimized in the gas phase at B3LYP/LanL2DZ level of theory without any constraint.[16] The structures of free ligand (**1**) was also fully optimized at the same level of theory. Natural bond orbital (NBO) calculations were performed with the NBO code included in Gaussian03 program[17] at B3LYP/LanL2DZ level of theory.
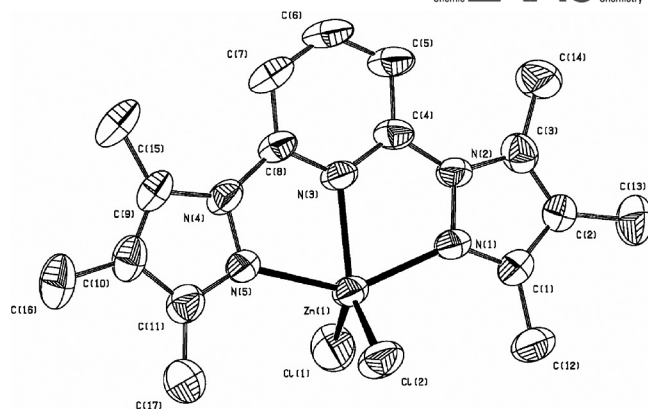

Figure 2. Molecular structure of complex **2**, showing 40 % probability displacement ellipsoids and the atom-numbering scheme.
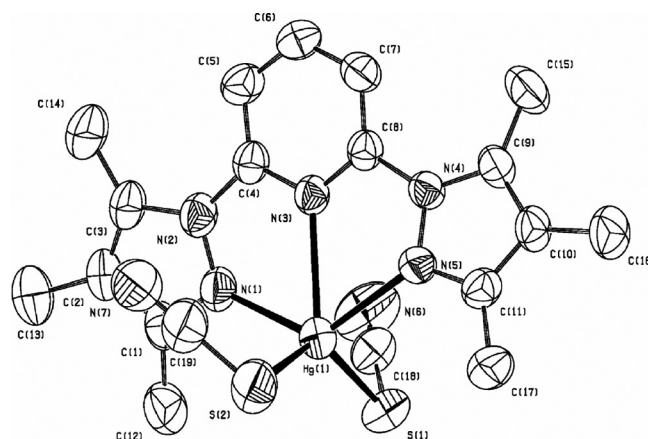

Figure 3. Molecular structure of complex **3**, showing 40 % probability displacement ellipsoids and the atom-numbering scheme.

Results and Discussion

FT-IR Spectroscopy

To study coordination of the ligand btmpp to zinc and mer-cury atoms in the complexes, the IR spectrum of the free li-gand was compared with the IR spectra of **2** and **3**. The interest in the IR spectrum of complex **3** is mainly due to the bands of the SCN$^-$ ion around 2119 cm^{-1}. The FT-IR spectrum of the free ligand shows weak bands at 2859, 2918 cm^{-1}, and 3087 cm^{-1}, which can be assigned to CH$_3$ and aromatic hydro-gen bonds. However, the band at 1599 cm^{-1} in the free ligand is shifted to 1611 cm^{-1} in **2** and 1604 cm^{-1} in **3**, indicating a non-coordinated pyridine ring,[18] this fact, together with the shifts of γ(CH) and δ(ring) in the spectrums may also indicate interaction between the zinc and mercury atoms and the pyri-dine ring. The ν(C=N) vibration of the pyrazole ring at 1583 cm^{-1} in the free ligand is shifted to 1575 cm^{-1} in **2** and to 1577 cm^{-1} in **3**. The FT-IR spectrum of the thiocyanate an-ion for complex **3** shows characteristic very strong absorption bands ν_{asy}(C=N) at 2119 cm^{-1}, due to the presence of the ter-minal thiocyanato ligands. The bands at 583, 602, 614 cm^{-1} for **2**, and 573, 599, 626 cm^{-1} for **3**, which are absent in **1**, can

Table 1. Crystal data and experimental details of complexes **2** and **3**.

	$C_{17}H_{21}Cl_2N_5Zn$ (**2**)	$C_{19}H_{21}HgN_7S_2$ (**3**)
Chemical Formula	$C_{17}H_{21}Cl_2N_5Zn$ (**2**)	$C_{19}H_{21}HgN_7S_2$ (**3**)
Formula weight	431.66	612.14
Crystal system	Monoclinic	Monoclinic
Space group	$P2_1/c$	$P2_1/c$
a /Å	7.9722(6)	8.7830(3)
b /Å	18.3084(13)	21.1489(7)
c /Å	13.3117(9)	12.0682(4)
β /°	97.504(6)	98.351(3)
Unit cell volume V /Å^3	1926.3(2)	2217.91(13)
Z	4	4
Calculated density D_x /g·cm^{-3}	1.488	1.833
Electron number $F(000)$	888	1184
Linear absorption coefficient μ /mm^{-1}	1.562	7.148
Crystal color, shape	Colorless, needle	Colorless, prism.
Crystal dimensions /mm	0.19 × 0.32 × 0.41	0.16 × 0.35 × 0.59
X-ray and wavelength	Mo-K_α, 0,71073	Mo-K_α, 0,71073
Data collection temperature, T /K	293(2)	293(2)
R_{int}	0.179	0.160
h, k, l intervals /°	−10/10, −19/23, −16/16	−11/11, −26/26, −15/15
$\theta_{max.}$ /°	26.85	27.30
Data collection device	STOE IPDS 2	STOE IPDS 2
Reflections with $(I > 2\sigma(I))$	2201	4058
Measured reflections	11098	33594
Independent reflections	4077	4718
Parameter number	233	261
$R, R_W(I > \sigma(I))$	0.074, 0.196	0.043, 0.103
S	0.99	1.10
$\Delta\rho_{min.}, \Delta\rho_{max.}$ /e·Å^{-3}	1.04, −0.57	1.03, −1.94

be assigned to the *M*–N frequencies, which is in agreement with the reported frequencies for similar compounds.[19]

Absorption Spectroscopy

The absorption spectra of the ligand (btmpp) and complexes **2** and **3** were recorded in dimethylformamide. The UV spectra for ligand and complexes showed two strong absorptions bands between 265 and 303 nm. For complex **2** and **3**, two bands occurred near 273 nm (13000 м$^{-1}$·cm^{-1}), 303 nm (15000 м$^{-1}$·cm^{-1}), and 266 nm (15000 м$^{-1}$·cm^{-1}), 302 nm (18000 м$^{-1}$·cm^{-1}), respectively. The spectrum of the free ligand exhibits intense peaks at 265 nm (12600 м$^{-1}$·cm^{-1}) and 303 nm (17500 м$^{-1}$ cm^{-1}), which indicate ligand-centered bands in this region, though other charge-transfer transitions also may contribute significantly to the intensity. The relative intensities of these bands were lower than those of the free ligand. A similar observation was mentioned by *Willison* et al.[8] For comparison, coordination of 2,2'-bipyridine to an acidic metal atom is known to result in intense and structured π–π* absorption in the vicinity of 290–310 nm, which is very different from the spectrum of the free ligand.[20]

Figure 4 shows the energy levels and the distributions of the HOMO-1, HOMO, LUMO and LUMO+1 orbitals calculated at B3LYP/LanL2DZ level of theory for **1**, **2** and **3**. One can see that nearly all the MOs are substantially localized on conjugate plane, with only small contributions to the group out of plane in the free ligand, **1**. However, HOMO-1 and HOMO orbitals are substantially localized on chlorido ions and thiocyanato ions, especially the π-bonding orbitals of sulfur atoms, of com-

plexes, **2** and **3**, respectively. The LUMO, LUMO+1 orbitals are mainly confined in the btmpp part of the metal complexes. Moreover, the frontier molecular orbital energies play an important role in the electric and optical properties, as well as in UV/Vis spectra and chemical reactions in the conjugated molecules.[21] The HOMO–LUMO energy gap of free ligand is 0.177 eV, whereas that of **2** and **3** are 0.111 and 0.112 eV, respectively, allowing electron movement between these orbitals to easily occur so that a peak around 250–310 nm can be observed in the UV/Vis spectrum.

Crystal Structures of the Complexes

The ORTEP and molecular packing diagrams of the monomeric unit of compound **2** are shown in Figure 2, Figure 3, Figure 4, and Figure 5, respectively. The crystal data collection and refinement of **2** are summarized in Table 1 and the important bond lengths and bond angles are listed in Table 2. It crystallizes in space group $P2_1/c$. One neutral tridentate molecule and two chlorido ligands are coordinated to the Zn^{II} ion in pentacoordinate environment. In pentacoordinated compounds the coordination sphere can be described either as square-pyramidal or trigonal bipyramidal depending on the parameter $\tau = (\beta - \alpha) / 60$ (α and β are the two largest bond angles around the metal ion). Generally, for an ideal square pyramidal arrangement $\tau = 0$ and for an ideal trigonal bipyramidal arrangement $\tau = 1$.[22] The largest bond angles in the coordination sphere are 143.0(2) [N5–Zn–N1] and 125.70(15) [N3–Zn–Cl2], which give a τ value of 0.288. This value is closer to that of a distorted square-pyramid around the zinc atom. The mean
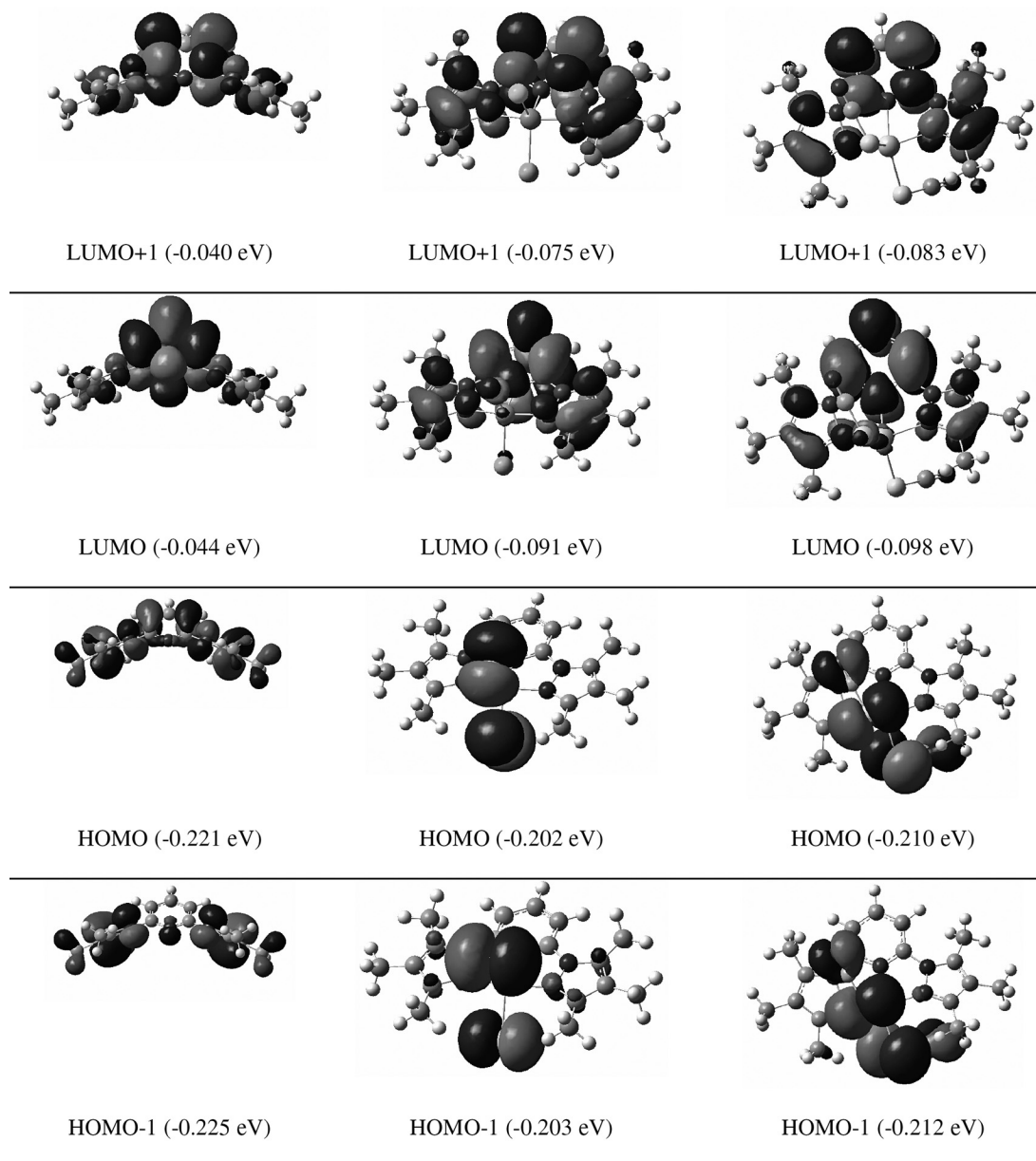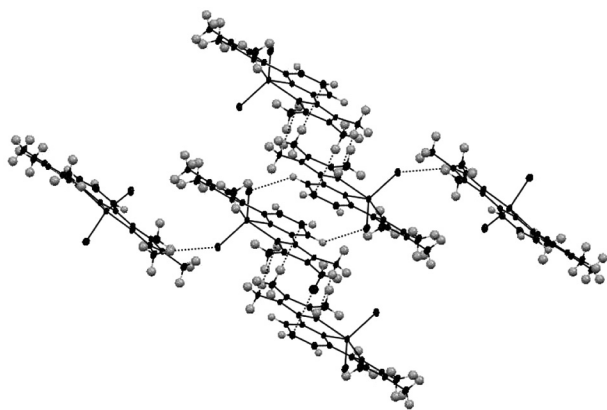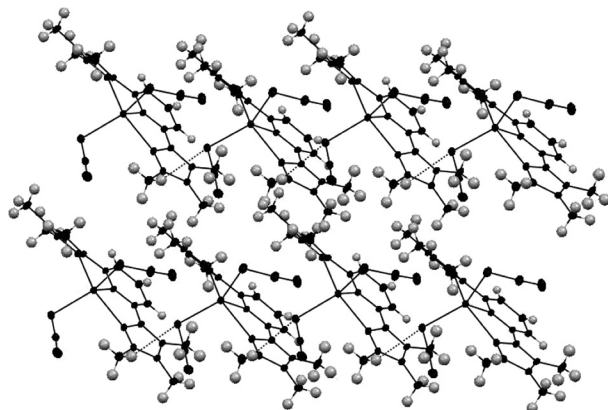
LUMO+1 (-0.040 eV)   LUMO+1 (-0.075 eV)   LUMO+1 (-0.083 eV)

LUMO (-0.044 eV)   LUMO (-0.091 eV)   LUMO (-0.098 eV)

HOMO (-0.221 eV)   HOMO (-0.202 eV)   HOMO (-0.210 eV)

HOMO-1 (-0.225 eV)   HOMO-1 (-0.203 eV)   HOMO-1 (-0.212 eV)

Figure 4. Selected HOMO and LUMO orbitals of compounds **1**–**3** and their energies (in parentheses). Positive values of the orbital contour are represented in light grey (0.04 au) and negative values in dark grey (–0.04 au).

basal plane is occupied by the three nitrogen atoms (N3 from pyridine and N1, N5 from the pyrazole groups) and one chlorido atom (Cl2). The apical site is occupied by the other chlorido atom (Cl1).

The basal site bond lengths of Zn–N1, Zn–N3, Zn–N5, Zn–Cl2 amount to 2.168(5), 2.202(6), 2.159(5), and 2.260(2) Å, respectively and the Zn–Cl1 bond length of the apical site amounts to 2.236(2) Å. The equatorial bond angles N1–Zn–N3, N3–Zn–N5, N1–Zn–Cl2 and N1–Zn–Cl1 are 71.4(2), 71.8(2), 98.43(16), and 99.98(16), respectively. The zinc atom is deviated from the mean basal plane by N1, N3, N5 and Cl2 by 0.712 Å. This deviation from the square pyramidal geometry is indicated by the equatorial bond angles that vary from 71.4(2) to 99.98(16)° from its normal value of 90°. The *trans*

angles N3–Zn1–Cl2 and N5–Zn1–N1 have values of 125.69(16) and 143.0(2), respectively and are not close to linearity.

Crystal data collection and refinement of compound **3** are summarized in Table 1. The ORTEP and molecular packing diagrams are displayed in Figure 3 and Figure 6, respectively. Selected bond lengths and angles in **3** are listed in Table 2. Compound **2** crystallizes in space group $P2_1/c$. The pentacoordinate Hg^{II} atom in **3** adopts a distorted square-pyramidal arrangement and is coordinated by three nitrogen atoms from the btmpp ligand and two sulfur atoms from the thiocyanate ions. The largest bond angles in the coordination sphere are 127.97(8)° [S2–Hg1–S1] and 126.83(16)° [N1–Hg1–N5], which give a τ value of 0.019. This value is closer to distorted

Figure 5. Packing diagram of [Zn(btmpp)Cl₂].

Figure 6. Packing diagram of [Hg(btmpp)(SCN)₂].

square-pyramidal arrangement around the mercury atom. The mean basal plane is occupied by the two nitrogen atoms (N1, N5 from the pyrazole groups) and two sulfur atoms (from thiocyanate ions). The apical site is occupied by the pyridine nitrogen atom. The thiocyanate ions are almost linear coordinated with N6–C18–S1 and N7–C19–S2 bond angles of 176.4(7)° and 177.1(9)°, respectively. All bond lengths and angles are

Table 3. Hydrogen bonding geometry /Å, °

	D–H⋯A	D–H	H⋯A	D⋯A	D–H⋯A
Hgbtmpp(SCN)₂*	C5–H5⋯N6ⁱ	0.93	2.50	3.327(10)	148
	C7–H7⋯N7ⁱⁱ	0.93	2.62	3.469(10)	151
	C12–H12C⋯S1ⁱⁱⁱ	0.96	2.96	3.750(10)	140
ZnbtmppCl₂**	C17–H17B⋯Cl1ⁱ	0.96	2.77	3.722(10)	172

Table 2. Selected bond lengths /Å, bond angles and dihedral angles /° for compounds, **1**–**3** (*M* = Zn, Hg and *X* = Cl, S).

	1 (free ligand)	**2** (Zn)		**3** (Hg)	
Bond lengths	calculated	calculated	measured	calculated	measured
N1–N2	1.398	1.401	1.379	1.404	1.355
N2–C4	1.424	1.412	1.406	1.414	1.407
C4–N3	1.349	1.351	1.328	1.352	1.347
C4–C5	1.412	1.410	1.379	1.409	1.385
C5–C6	1.404	1.403	1.389	1.401	1.378
N2–C3	1.380	1.405	1.380	1.401	1.395
M–N1	–	2.193	2.168	2.545	2.428
M–N3	–	2.238	2.202	2.514	2.532
M–N5	–	2.193	2.158	2.504	2.433
M–*X*1	–	2.351	2.236	2.685	2.444
Bond angles					
N1–N2–C4	119.35	116.75	116.21	118.29	118.74
N1–N2–C3	111.83	110.17	110.09	110.59	109.71
N2–C3–C14	123.86	125.13	123.90	124.82	124.98
N2–C4–C5	120.03	124.67	124.63	122.80	124.29
C4–N3–C8	118.58	121.40	120.39	120.75	118.20
C4–C5–C6	118.09	117.42	116.66	117.85	117.66
C1–C2–C3	105.70	106.39	105.46	106.23	106.32
N1–*M*–N3	–	71.74	71.42	64.40	63.42
N1–*M*–N5	–	142.46	142.95	128.68	126.80
N3–*M*–*X*1	–	128.28	125.69	102.32	114.58
Dihedral angles					
N1–N2–C4–N3	48.12	2.64	12.15	17.56	10.79
N5–N4–C8–N3	48.11	2.63	1.64	21.88	16.91
C1–C2–C3–C14	177.28	179.45	178.81	171.95	177.68
C4–C5–C6–C7	1.15	0.09	1.01	1.89	0.32
N3–*M*–N1–N2	–	7.66	10.69	28.32	19.18
Dipole moment	5.48	12.89	–	9.10	–

in agreement with those in similar structures.[23,24] Hydrogen bonding geometry is shown in Table 3. The asymmetric unit of the title compound contains two crystallographically independent molecules, and the molecules exist as C5–H5···N6 and C7–H7···N7 hydrogen-bonded centrosymmetric dimers with $R_2^2(16)$, $R_2^2(16)$ rings, respectively. Analysis of the crystal packing of the title compound reveals that the molecules are linked by weak π···π stacking interaction between the centroids of the N3–C8 rings [Cg···Cg (2–x, –y, 1–z) = 3.747(3) Å].

In general, the predicted bond lengths and angles are in agreement with the values based upon the X-ray crystal structure data, and the general trends observed in the experimental data are well reproduced in the calculations.

Thermal Analyses

TG and DTA analyses of the complex **2** were carried out under inert atmosphere. As the results obtained from the TGA-DTA thermogram of **2** showed, no weight loss occurred up to 300 °C (Figure 7). The complex started to melt at 358 °C. It was observed that during melting the complex also started to decompose. Between 300–900 °C, it could be conceived that a mass loss of 84.7 % with a large thermal decomposition belongs to the btmpp ligand and two chlorine atoms because the ratio of the bdmpp ligand and chlorine atoms in the complex amounts to 84.9 %. The second endothermic peak of the DTA curve was due to this decomposition. At 900 °C a residue of 15.3 % remained, which might be metallic zinc (theoretical value: 15,3 %). At higher temperatures weight loss continued slowly, which might be explained by sublimation of zinc.
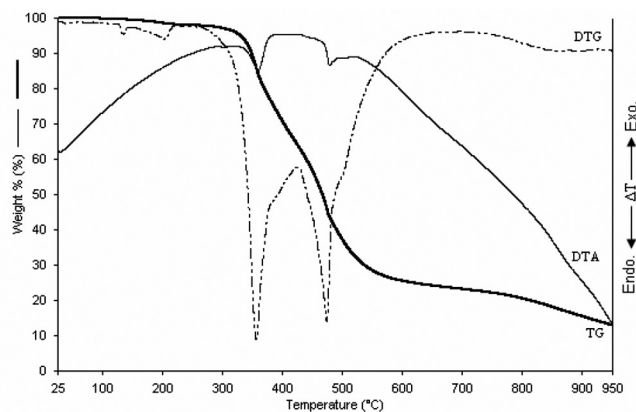

Figure 7. DTA/TG curves of [Zn(btmpp)Cl₂].

Complex **3** is stable up to 250 °C (Figure 8). Three endothermic and one exothermic signals were observed in the DTA curve. The first endothermic peak at 178 °C is due to melting of the complex. Thermal decomposition of complex **3**, took place in three steps. In the first step a weight loss of 49.5 % was observed between 200–330 °C, which corresponds with the btmpp ligand ratio in complex **3**. Between 330 °C–420 °C a weight loss of 35,8 % was observed, which might be due to the leave of HgS (in theoretical 37.9 %). Up to a temperature

of 850 °C, the mass nearly vanishes. This situation shows that rest of the structure mainly sublimes in the final decomposition step.
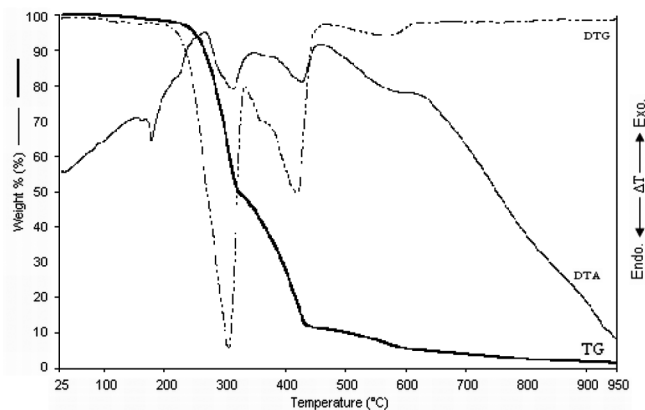

Figure 8. DTA/TG curves of the [Hg(btmpp)(SCN)₂].

Charge Distributions

Table 4 shows the atomic charges from natural population analyses (NPA) for **1**–**3**. The calculated charges on the metal ions, zinc and mercury are considerable lower than the formal charge, +2. The population of the p_x, p_y, and p_z orbitals of the metal atoms in **2** and **3** are given in the following: complex **2**-Zn: 0.00766, 0.01400, and 0.01258 e; complex **3**-Hg: 0.00838, 0.00617, and 0.01198 e⁻. Moreover, the d_{xy}, d_{xz}, d_{yz}, $d_{x^2-y^2}$ and d_{z^2} orbitals of the metal atoms in **2** and **3** are occupied more than 1.99 e⁻. This is the result of significant charge donation from the btmpp ligand, chlorido ions and thiocyanato ions. The mercury ions in **3** are less positive in comparison with the zinc ions in **2**. In both complexes **2** and **3**, the considerably less negative values of charges are observed for btmpp ligand when compared with the charges of free ligand **1**. This indicates the higher electron delocalization from the N_1, N_3, and N_5 atoms towards the metal atoms zinc and mercury and corresponds to differences in the M–N bond lengths.

Table 4. Calculated NPA charges of optimized structures; **1**, **2**, and **3** at B3LYP/LanL2DZ level.

	1	2	3
N1	−0.291	−0.440	−0.428
N2	−0.268	−0.242	−0.244
N3	−0.461	−0.641	−0.615
N4	−0.268	−0.242	−0.247
N5	−0.291	−0.440	−0.432
M	–	1.582	1.413

NBO Analyses

The application of natural bond orbital (NBO) analysis has been described elsewhere.[25] A useful aspect of the NBO method is that it provides information about interactions in

both filled and virtual orbital spaces that could enhance the analysis of intra- and intermolecular interactions. Selected NBOs occupancies and energies for compounds **1**–**3** are listed in Table 5, which were calculated on natural atomic orbital and bond orbital analyses at B3LYP/LanL2DZ level based on the experimental structures.

Table 5. Selected NBOs occupancies and energies of compounds **1**–**3**.

NBO	1 Occupancy	Energies	2 Occupancy	Energies	3 Occupancy	Energies
LP N1	1.94681	–233,89	1.91590	–281,61	1.91212	–277,06
LP N2	1.57947	–160,83	1.56877	–187,67	1.56763	–186,13
LP N3	1.90467	–200,70	1.89312	–252,43	1.87848	–248,06
LP N4	1.57947	–160,83	1.56877	–187,67	1.57405	–189,19
LP N5	1.94681	–233,89	1.91590	–281,61	1.90410	–281,10
LP M	–	–	1.99958	–355,96	1.99897	–342,34
LP M	–	–	1.99809	–354,83	1.99812	–342,29
LP M	–	–	1.99805	–355,02	1.99753	–341,92
LP* M	–	–	0.38456	28,44	0.56541	–82,51

LP represents lone pair, LP* represents *anti*-LP. Energies in kcal·mol^{-1}.

NBO analyses revealed that the electronic occupancies of the *anti*-LP electrons of **3** are distinctly higher than those of **2** and the orbital potential energy of the *anti*-LP electrons of **3** are lower than those of **2**. The electronic populations on the lone pair orbitals of nitrogen atoms have an occupation significantly lower than two electrons. The low occupancies of the p orbitals of nitrogen atoms support the idea of the presence of delocalized bonds between the "π" molecular orbital of the nitrogen lone pair in the plane of btmpp ligand and the molecular orbital of the zinc and mercury atoms in this plane. At the same time, according to the results of second order perturbation theory analyses not reported here, the lone pairs of metal atoms in **2** and **3** have no contribution to the coordination of the compounds.

Conclusions

This study aimed to obtain and discover monomeric complexes of btmpp. Btmpp-metal complexes have been only rarely reported in literature. The ligand btmpp and its Zn^{II} and Hg^{II} complexes were synthesized and characterized by single-crystal X-ray diffraction, elemental analysis, thermal analysis, and ^{1}H NMR, ^{13}C NMR, IR, and UV/Vis spectroscopy.

The structures of complexes, **2** and **3**, computed at the B3LYP/ LanL2DZ level of theory agreed well with experiment values obtained from their X-ray analyses. Computational studies from NBO analyses also depicted that in both complexes **2** and **3**, the considerable differences in values of charges for the ligand btmpp became less negative when compared with the charges of free ligand **1**.

Acknowledgement

References

[1] M. Loi, M. W. Hosseini, A. Jouaiti, A. De Cian, J. Fischer, *Eur. J. Inorg. Chem.* **1999**, 1981–1985.

[2] K. Chryssou, V. J. Catalano, R. Kurtaran, P. Falaras, *Inorg. Chim. Acta* **2002**, *328*, 204–209.

[3] B. Çetinkaya, E. Çetinkaya, M. Brookhart, P. S. White, *J. Mol. Catal. A* **1999**, *142*, 101–112.

[4] D. J. Hathcock, K. Stone, J. Madden, S. J. Slattery, *Inorg. Chim. Acta* **1998**, *282*, 131–135.

[5] P. Manikandan, R. Muthukumaran, K. R. J. Thomas, B. Varghese, G. V. R. Chandramouli, P. T. Manoharan, *Inorg. Chem.* **2001**, *40*, 2378–2389.

[6] Z. Yongbo, Z. Xiaoming, C. Wanzhi, Q. Huayu, *J. Organomet. Chem.* **2008**, *693*, 205–215.

[7] M. J. Graneto, R. G. Kurumbail, M. L. Vazquez, H. S. Shieh, J. L. Pawlitz, J. M. Williams, W. C. Stallings, L. Geng, A. S. Naraian, F. J. Koszyk, M. A. Stealey, X. D. Xu, R. M. Weier, G. J. Hanson, R. J. Mourey, R. P. Compton, S. J. Mnich, G. D. Anderson, J. B. Monahan, R. Devraj, *J. Med. Chem.* **2007**, *50*, 5712–5719.

[8] S. A. Willison, H. Jude, R. M. Antonelli, J. M. Rennekamp, N. A. Eckert, J. A. Krause Bauer, W. B. Connick, *Inorg. Chem.* **2004**, *43*, 2548–2555.

[9] K. Guzow, M. Milewska, C. Czaplewski, W. Wiczk, *Spectrochim. Acta Part A* **2010**, *75*, 773–781.

[10] C. Hopa, M. Alkan, C. Kazak, N. B. Aslan, R. Kurtaran, *Transition Met. Chem.* **2009**, *34*, 403–407.

[11] C. Hopa, M. Alkan, C. Kazak, N. B. Aslan, R. Kurtaran, *J. Chem. Crystallogr.* **2009**, *40*, 160–164.

[12] E. Lopez-Torres, M. A. Mendiola, J. Rodriguez-Procopio, M. T. Sevilla, E. Colacio, J. M. Moreno, I. Sobrados, *Inorg. Chim. Acta* **2001**, *323*, 130–138.

[13] H. R. Khavasi, A. Abedi, A. Amani, V. Amani, B. Notash, N. Safari, *Polyhedron* **2008**, *27*, 1848–1854.

[14] G. M. Sheldrick, *SHELXS-97 and SHELXL-97*, Programs for Crystal Structure Analysis, University of Göttingen, Germany, **1997**.

[15] L. J. Farrugia, *J. Appl. Crystallogr.* **1999**, *30*, 565.

[16] F. Jensen, *Introduction to Computational Chemistry*, Wiley, UK, **1999**.

[17] M. J. Frisch, G. W. Trucks, H. B. Schlegel, G. E. Scuseria, M. A. Robb, J. R. Cheeseman, J. A. Montgomery, T. Vreven, K. N. Kudin, J. C. Burant, J. M. Millam, S. S. Iyengar, J. Tomasi, V. Barone, B. Mennucci, M. Cossi, G. Scalmani, N. Rega, G. A. Petersson, H. Nakatsuji, M. Hada, M. Ehara, K. Toyota, R. Fukuda, J. Hasegawa, M. Ishida, T. Nakajima, Y. Honda, O. Kitao, H. Nakai, M. Klene, X. Li, J. E. Knox, H. P. Hratchian, J. B. Cross, V. Bakken, C. Adamo, J. Jaramillo, R. Gomperts, R. E. Stratmann, O. Yazyev, A. J. Austin, R. Cammi, C. Pomelli, J. W. Ochterski, P. Y. Ayala, K. Morokuma, G. A. Voth, P. Salvador, J. J. Dannenberg, V. G. Zakrzewski, S. Dapprich, A. D. Daniels, M. C. Strain, O. Farkas, D. K. Malick, A. D. Rabuck, K. Raghavachari, J. B. Foresman, J. V. Ortiz, Q. Cui, A. G. Baboul, S. Clifford, J. Cioslowski, B. B. Stefanov, G. Liu, A. Liashenko, P. Piskorz, I. Komaromi, R. L. Martin, D. J. Fox, T. Keith, Al M. A. Laham, C. Y. Peng, A. Nanayakkara, M. Challacombe, P. M. W. Gill, B. Johnson, W. Chen, M. W. Wong, C. Gonzalez, J. A. Pople, *Gaussian 03*, Revision C02, Gaussian Inc., Pittsburgh PA, **2003**.

[18] F. Ercan, C. Arici, D. Ulku, R. Kurtaran, M. Aksu, O. Atakol, *Z. Kristallogr.* **2004**, *219*, 295–299.

[19] K. Nakamato, *The Infrared Spectra of Inorganic and Complex Molecules*, John Wiley and Sons, Inc., **1982**.

[20] a) R. G. Bray, J. Ferguson, C. J. Hawkins, *Aust. J. Chem .* **1969**, *22*, 2091; b) T. Ohno, S. Kato, *Bull. Chem. Soc. Jpn.* **1974**, *47*, 2953.

[21] a) I. Fleming, *Frontier Orbitals and Organic Chemical Reactions*, Wiley, London, **1976**; b) L. Turker, A. Azizoglu, *THEOCHEM* **2001**, *535*, 151; c) A. Azizoglu, *Struct. Chem.* **2003**, *14*, 575.

[22] A. W. Addison, R. T. Nageswara, J. Reedijk, J. Van Rijn, G. J. Verschoor, *J. Chem. Soc., Dalton Trans.* **1984**, 1349–1355.

[23] R. Kurtaran, S. Odabaşıoğlu, A. Azizoğlu, H. Kara, O. Atakol, *Polyhedron* **2007**, *26*, 5069–5074.

[24] M. Taştekin, C. Arıcı, I. Svoboda, K. C. Emregül, R. Kurtaran, O. Atakol, H. Fuess, *Z. Kristallogr.* **2007**, *222*, 255–258.

[25] a) A. E. Reed, L. A. Curtius, F. Weinhold, *Chem. Rev.* **1988**, *88*, 899–926; b) A. E. Reed, P. v. R. Schleyer, *J. Am. Chem. Soc.* **1990**, *112*, 1434–1445; c) D. Margetic, Y. Murata, K. Komatsu, *Struct. Chem.* **2007**, *18*, 279–286; d) A. Azizoglu, M. Balci, J. L. Mieusset, U. Brinker, *J. Org. Chem.* **2008**, *73*, 8182–8188; e) B. Kilbas, A. Azizoglu, M. Balci, *J. Org. Chem.* **2009**, *74*, 7075–7083; f) G. Alpaslan, H. Tanak, A. A. Agar, A. Erdönmez, Ş. Işık, submitted DOI: 10.1007/s1122401096417

———————————